
Towards Neural Sparse Linear Solvers

Luca Grementieri¹ Paolo Galeone¹

Abstract

Large sparse symmetric linear systems appear in several branches of science and engineering thanks to the widespread use of the finite element method (FEM). The fastest sparse linear solvers available implement hybrid iterative methods. These methods are based on heuristic algorithms to permute rows and columns or find a preconditioner matrix. In addition, they are inherently sequential, making them unable to leverage the GPU processing power entirely. We propose neural sparse linear solvers, a deep learning framework to learn approximate solvers for sparse symmetric linear systems. Our method relies on representing a sparse symmetric linear system as an undirected weighted graph. Such graph representation is inherently permutation-equivariant and scale-invariant, and it can become the input to a graph neural network trained to regress the solution. We test neural sparse linear solvers on static linear analysis problems from structural engineering. Our method is less accurate than classic algorithms, but it is hardware-independent, fast on GPUs, and applicable to generic sparse symmetric systems without any additional hypothesis. Although many limitations remain, this study shows a general approach to tackle problems involving sparse symmetric matrices using graph neural networks.

1. Introduction

The resolution of linear systems is a classical problem at the core of the numerical analysis. Linear systems are so pervasive because they are a fundamental component of the numerical resolution of differential equations. For this reason, they appear in all branches of science: from engineering to biology. The finite element method (FEM) is a popular and accurate method to solve differential equations numerically (Logan, 2016). In this context, the matrix as-

sociated with the linear system has the property to be very sparse and symmetric (and often positive-definite). The real-time simulation of FEM models requires fast resolution algorithms that can be inaccurate up to a certain degree. Classic methods to solve sparse linear systems have been conceived before the introduction of GPGPU computing when the processing power available was very limited, so they are not suited to use a GPU effectively. The methods to solve sparse linear systems are classified into direct and iterative methods.

Direct methods, also known as decomposition methods, rely on a factorization of the coefficient matrix in a pair of matrices that have simplifying properties, like triangular or orthogonal matrices. The most established direct methods are LU factorization (equivalent to Cholesky decomposition for definite-positive matrices) and QR decomposition. Decomposition methods are very accurate, but their parallelization on modern hardware (GPUs) is complicated, and it is impossible to trade off accuracy for computational time. Moreover, the factors obtained in the decomposition process can be much less sparse than the starting matrix, causing an increase in memory consumption. Every null element of the initial matrix that becomes a non-null value during the factorization is called a *fill-in*. When the number of fill-ins is large, the execution time increases considerably because the mutation of the sparsity pattern of a sparse matrix is a slow operation. A permutation of rows and columns can mitigate the appearance of fill-ins by concentrating the non-null elements of the sparse matrix around the diagonal. The research of the optimal permutation that minimizes the number of fill-ins is an NP-hard problem (Yannakakis, 1981), so heuristic fill-reducing algorithms are employed in practice.

Iterative methods repeatedly refine an approximate solution starting from an initial guess, often the null vector. Iterative methods have the advantage that a less stringent stopping criterion permits the reduction of the execution time at the expense of a less accurate solution. The coefficient matrix is never changed or inverted, but it is used only to perform matrix-vector multiplications. For this reason, iterations are fast on GPU but, since these methods are inherently sequential, the GPU usage is low, and the degree of parallelization is limited. When the condition number of the coefficient matrix is high, iterative methods can incur a slow convergence increasing the total computation time. Preconditioning meth-

¹ZURU Tech, Modena, Italy. Correspondence to: Luca Grementieri <luca.g@zuru.tech>.

ods are harnessed to reduce the condition number, but they can be slow on GPUs because they often rely on decomposition methods. The most adopted iterative methods are Conjugate Gradient (CG) or its variant Preconditioned Conjugate Gradient (PCG). Such algorithms are only applicable to positive-definite matrices. When the coefficient matrix is indefinite, it is possible to employ BiCGSTAB (Van der Vorst, 1992) or GMRES (Saad & Schultz, 1986), but they are often slower than CG on systems of similar size.

We are interested in fast approximate solvers that can be used in real-time non-critical applications to predict a coarse solution of a linear system. We present a deep learning framework to learn approximate sparse linear solvers tailored for a specific use case. Our approximate solvers hinge on the recent advances in graph neural networks (GNNs) and geometric deep learning (Bronstein et al., 2017). To leverage GNNs, we present a novel way to represent a sparse symmetric linear system as a weighted undirected graph. Using this input representation, we can cast the resolution of a sparse linear system as a node regression task. We tackle this regression task using a graph convolution network (GCN) coupled with some techniques to exploit the scale invariance property of the problem.

We test our neural sparse linear solvers (NSLSs) on a dataset of synthetic and realistic symmetric positive-definite linear systems coming from the field of structural engineering. Our tests show that our approximate solver is less accurate than existing methods and, for this reason, slower if compared with other iterative methods (being the relative error equal). Nevertheless, an NSLS has several advantages: it does not suffer from convergence issues caused by ill-conditioned matrices; its implementation is hardware-independent; the training on positive-definite, indefinite, or general sparse symmetric systems does not require any change.

Lastly, we consider our proposed deep learning approach an initial significant example of how deep learning can help solve numerical analysis problems on sparse matrices. Our technique is part of the broader line of research toward computational-aided mathematics (Lample & Charton, 2019; Davies et al., 2021).

To summarize, our contributions are the following:

- we introduce a novel representation of a sparse symmetric linear system as a weighted undirected graph;
- we frame the resolution of a sparse linear system as a node regression task;
- we build a GNN-based deep learning model to solve approximately linear systems.

2. Background

2.1. Problem Definition

Let Sym_n be the set of real symmetric $n \times n$ matrices. A symmetric linear system is defined by a symmetric matrix of coefficients $A \in Sym_n$ and the vector of constant terms $\mathbf{b} \in \mathbb{R}^n$. The solution of the linear system is the vector $\mathbf{x} \in \mathbb{R}^n$ such that

$$A\mathbf{x} = \mathbf{b}. \quad (1)$$

A system is said *sparse* if A is a sparse matrix, i.e. the number of non-zero entries scales linearly with the number of rows and columns.

If $\det(A) \neq 0$, the linear system (1) has a unique solution, so it exists a solution function s that maps the linear system to its solution

$$s(A, \mathbf{b}) = A^{-1}\mathbf{b} = \mathbf{x}. \quad (2)$$

s is linear with respect to \mathbf{b} , but it is non-linear with respect to A because matrix inversion is a non-linear operation.

The computation of s is slow when n is large, so we look for an algorithm to approximate the function s .

2.2. Preconditioning

One possibility is to approximate the inversion of A separating the linear part of s , the multiplication with \mathbf{b} from the non-linear inversion of A . The line of research that proposes new preconditioning methods follows this approach implicitly.

A *preconditioner* M of a matrix A is a matrix such that $M^{-1}A$ has a smaller condition number than A (and M^{-1} is easy to compute). When a preconditioner M is available, the solution \mathbf{x} is computed solving the equivalent system $M^{-1}A\mathbf{x} = M^{-1}\mathbf{b}$. For a symmetric matrix A (a special case of a normal matrix), the condition number is

$$\kappa(A) = \|A^{-1}\| \cdot \|A\| = \frac{|\lambda_{\max}(A)|}{|\lambda_{\min}(A)|} \geq 1,$$

where $\lambda_{\max}(A)$ and $\lambda_{\min}(A)$ are maximal and minimal (by modulus) eigenvalues of A respectively. It follows that the minimum condition number is attained on multiples of the identity matrix.

Preconditioning methods try to approximate the inverse of A under some restrictive conditions to minimize the condition number. For example, usually, the sparsity pattern of M or M^{-1} coincides with the sparsity pattern of A . With such limitation, the inverse A^{-1} can be approximated but not recovered because the inverse matrix of a sparse matrix is non-sparse in the general case. The methods that learn the preconditioning method based on a dataset of matrices often impose the same sparsity constraint (Götz & Anzt, 2018).

3. Graph Representation of a Sparse System

In this work, we propose a method to approximate the function s directly using a neural network. Before applying any model, we have to represent the sparse system in a form appropriate to input it into a neural network model.

Rose (1972) shows that a sparsity profile of a symmetric matrix can be described by an undirected graph between n nodes. Starting from this idea, we define the graph \mathcal{G} associated with a symmetric sparse linear system.

An *undirected graph* \mathcal{G} is a pair (V, E) composed of a finite set of nodes V and a set of undirected edges $E \subseteq \{\{u, v\} \subseteq V\}$. A *weighted graph* additionally associates to every edge $e \in E$ a real value $w(e)$, called its *weight*. The *adjacency matrix* of a weighted undirected graph is a symmetric matrix $G \in \text{Sym}_n$ such that $g_{ij} = g_{ji} = w(\{i, j\})$ if $\{i, j\} \in E$, otherwise $g_{ij} = 0$. Thus, we can interpret any symmetric sparse matrix as the adjacency matrix of a weighted undirected graph \mathcal{G} .

In our graph representation of a sparse linear system, the coefficients in A become the weights of the undirected edges of the graph \mathcal{G} and every node of \mathcal{G} represent at the same time a variable of the system and one of its equations. The order of equations in a linear system does not influence its solution, so there is no canonical ordering in general. Nevertheless, when the matrix is symmetric, the order of equations (i.e. the order of rows in the matrix) and the order of variables (i.e. the order of columns in the matrix) are linked by the symmetry property of the matrix. To complete the representation of the system as a graph, we use the elements of \mathbf{b} as node features. In summary, as depicted in Figure 1, the i^{th} node of the graph \mathcal{G} is described by the feature b_i and it is linked to the j^{th} node if and only if $a_{ij} \neq 0$. If $a_{ij} \neq 0$, then the undirected edge e_{ij} is associated to the weight a_{ij} .

Apart from being more suitable to apply deep learning methods to the resolution of the problem, the graph representation is also inherently permutation-equivariant. It implies that an identical graph representation encodes symmetric systems obtained through permutations. This property is highly desirable because, if P is a permutation matrix, then the system $A\mathbf{x} = \mathbf{b}$ is equivalent to the system

$$(PAP^\top)\mathbf{y} = P\mathbf{b}, \text{ where } \mathbf{y} = P\mathbf{x} \text{ is a permutation of } \mathbf{x}.$$

On the contrary, the matrix representation of a linear system is not unique, and the order of rows and columns influences the resolution time of the linear system. For this reason, permutation heuristics try to find the most efficient form of a linear system.

Linear systems are also scale-invariant: in Section 4.2, we are going to explain how to scale edge weights and node features to represent scaled systems using the same graph.

$$\begin{pmatrix} 1.0 & 0.5 & 0 & 0 & 0 \\ 0.5 & 2.2 & 4.1 & 0 & 1.2 \\ 0 & 4.1 & -1.5 & 2.0 & 0 \\ 0 & 0 & 2.0 & 3.6 & -0.8 \\ 0 & 1.2 & 0 & -0.8 & -0.1 \end{pmatrix} \begin{pmatrix} x_1 \\ x_2 \\ x_3 \\ x_4 \\ x_5 \end{pmatrix} = \begin{pmatrix} 2.7 \\ -1.1 \\ -2.6 \\ 5.4 \\ 4.8 \end{pmatrix}$$

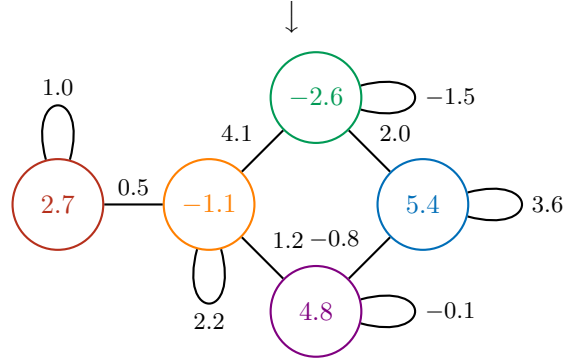


Figure 1. Conversion from the matrix representation to the graph representation of a sparse symmetric linear system.

4. Neural Sparse Solver

Equipped with the graph representation of a sparse linear system, we can now define our Neural Sparse Linear Solver (NSLS) model. An NSLS is a regression model that takes as input the graph associated with a sparse linear system according to the representation introduced in Section 3, and it outputs the approximate solution of the linear system. Three modules compose an NSLS: a feature augmentation module, a scaling module, and a graph neural network module. Such modules interact according to the workflow displayed in Figure 2.

4.1. Permutation-Equivariant Feature Augmentation

The naive application of a graph neural network on $\mathcal{G}_{A,\mathbf{b}}$ is prone to fail because every node stores a single scalar feature b_i . This description is insufficient to describe a node, so we need to enrich the node features and replace the scalar b_i with the feature vector \mathbf{f}_i .

Every permutation-equivariant operation involving A and \mathbf{b} that returns a vector $\mathbf{u} \in \mathbb{R}^n$, can be used to augment the features of the i^{th} node appending the value u_i to it. In practice, all features are normalized component-wise with the L_∞ norm to control the variance of the input passed to the graph neural network. The L_∞ norm is specifically chosen because it is independent of the size n .

The most simple augmentation is the *diagonal augmentation*: the value a_{ii} on the diagonal of the matrix A is added to the feature vector \mathbf{f}_i . To design other augmentation operations, we draw inspiration from existing iterative methods.

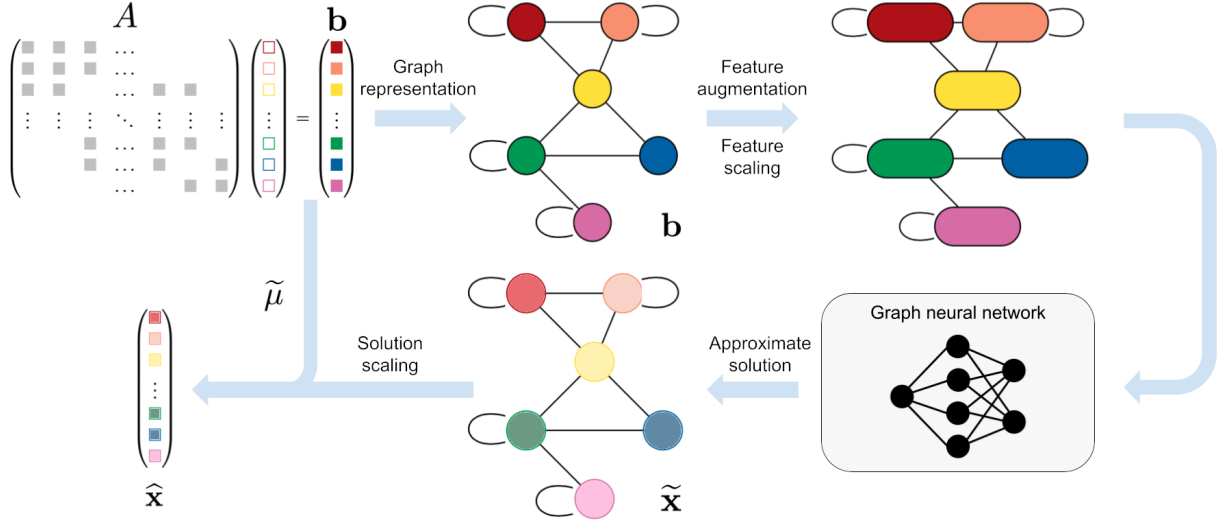


Figure 2. Structure of a Neural Sparse Linear Solver. The system is converted to a graph: the coefficient matrix defines the graph topology, and the constant term \mathbf{b} gives the node features. Node features are augmented with permutation-equivariant operations and scaled. A graph neural network takes this graph as input and predicts the direction of the approximate solution. Finally, the output of the graph neural network is scaled to minimize the residual vector.

Jacobi Augmentation. The Jacobi method is an iterative algorithm to solve the linear system $Ax = \mathbf{b}$ decomposing the matrix as $A = D + M$, where D is the diagonal matrix, and M is the sum of the lower and upper triangular parts. Jacobi iteration can be written as

$$\begin{cases} \mathbf{x}_{\text{Jacobi}}^{(0)} = \mathbf{0} \\ \mathbf{x}_{\text{Jacobi}}^{(k+1)} = D^{-1}(\mathbf{b} - M\mathbf{x}_{\text{Jacobi}}^{(k)}). \end{cases}$$

We append to the feature matrix F the vectors $\mathbf{x}_{\text{Jacobi}}^{(1)}, \dots, \mathbf{x}_{\text{Jacobi}}^{(m)}$ after normalization. The normalization here is necessary because the Jacobi iteration can diverge rapidly if the matrix A is not positive definite or strictly diagonally-dominant.

We could apply the same idea to similar iterative methods based on other decompositions of the matrix A , like Gauss-Seidel or SOR methods. Unfortunately, the iterations prescribed by these methods are not permutation-equivariant because the lower and upper parts of A are different from the corresponding parts of the permuted matrix PAP^T .

Conjugate Gradient Augmentation. A single iteration of the conjugate gradient method is a permutation-equivariant operation. Therefore, every conjugate gradient step provides values that can be appended element-wise to the corresponding node features. We expect this augmentation to be particularly effective when A is positive-definite, but it is still possible to apply it to general matrices.

Arnoldi Augmentation. Arnoldi iteration is described by

$$\mathbf{x}_{\text{Arnoldi}}^{(k)} = A^k \mathbf{b}.$$

The GMRES method (Saad & Schultz, 1986) is an iterative method for the numerical solution of a generic system of linear equations that relies on the Arnoldi iteration to approximate the solution. Thus, taking inspiration from GMRES, we enrich the node features appending the normalized version of the vectors $\mathbf{x}_{\text{Arnoldi}}^{(1)}, \dots, \mathbf{x}_{\text{Arnoldi}}^{(m)}$. Here, the permutation equivariance property of the augmentation comes from the orthogonality of permutation matrices. The normalization is crucial for Arnoldi augmentation because the repeated multiplication by A can easily cause overflows or underflows in the values of $\mathbf{x}_{\text{Arnoldi}}^{(k)}$.

The proposed augmentations can be combined to maximize the accuracy of the model. The number of elements added to the node features should balance accuracy gains with the increase in inference time. We compare the end-to-end performances obtained using every augmentation strategy and their combinations in Section 5.2.

4.2. Scale-Invariant Processing

The graph representation makes the model intrinsically permutation-equivariant: we now explain how to make the model scale-invariant. The scale invariance property allows us to describe entire classes of linear systems with a single representation, and it is even more critical for boosting model accuracy. Indeed, inputs of uncontrolled scale can hinder the training or make the model unstable and unreliable. Finally, scale invariance naturally helps generalization making it possible to manage solution vectors \mathbf{x} of different scales.

Let us notice that the system $A\mathbf{x} = \mathbf{b}$ is equivalent to

$$\mu \frac{A}{\|A\|} \frac{\mathbf{x}}{\|\mathbf{x}\|} = \frac{\mathbf{b}}{\|\mathbf{b}\|}, \text{ where } \mu = \frac{\|\mathbf{x}\| \|A\|}{\|\mathbf{b}\|},$$

for any norm $\|\cdot\|$ (or in general for every scaling factor). Let us denote the scaled quantities above as \bar{A} , $\bar{\mathbf{x}}$, $\bar{\mathbf{b}}$. If the normalized solution $\bar{\mathbf{x}}$ is known, we can recover

$$\mu = \frac{\|\bar{\mathbf{b}}\|_2}{\|\bar{A}\bar{\mathbf{x}}\|_2}.$$

If we only know an approximate scaled solution $\tilde{\mathbf{x}}$, then we can approximate μ as

$$\tilde{\mu} = \arg \min_{\mu} \|\mu \bar{A} \tilde{\mathbf{x}} - \bar{\mathbf{b}}\|_2^2.$$

The minimization problem has the closed-form solution

$$\tilde{\mu} = \frac{\langle \bar{A} \tilde{\mathbf{x}}, \bar{\mathbf{b}} \rangle}{\|\bar{A} \tilde{\mathbf{x}}\|_2^2}. \quad (3)$$

In conclusion, we can represent all scaled versions of a system canonically using the normalized coefficients \bar{A} and constant terms $\bar{\mathbf{b}}$. The model receives the system graph with scaled weights and features and, it predicts a scale-independent approximation of the solution $\tilde{\mathbf{x}}$. Hence, we recover the final approximate solution $\hat{\mathbf{x}}$ with the formula

$$\hat{\mathbf{x}} = \frac{\tilde{\mu} \|\mathbf{b}\|}{\|A\|} \tilde{\mathbf{x}}. \quad (4)$$

4.3. Graph Neural Network Backbone

The main component of an NSLS is a graph convolutional neural network (GCN) that maps the scaled augmented node features to the approximate direction of the solution. The GCN architecture follows the encode-process-decode model proposed by Battaglia et al. (2018): it is composed of a node encoder, followed by m residual blocks, and terminates with a solution decoder. The encoder is a linear layer, while the decoder is 2-layer MLP with LeakyReLU activation. The decoder outputs a single value per node, and all these values compose a permutation-equivariant description of the solution vector. For the residual block, we have tested many layers and their combinations to finally come up with the structure depicted in Figure 3.

Residual Connections. Li et al. (2020) empirically find that the pre-activation variant of residual connections for GCNs, which follows the ordering Normalization \rightarrow Activation \rightarrow GraphConv \rightarrow Addition, performs better than the standard ordering introduced by Li et al. (2019). Here, we use a similar design with an additional GraphConv layer between the normalization and the activation layers. The

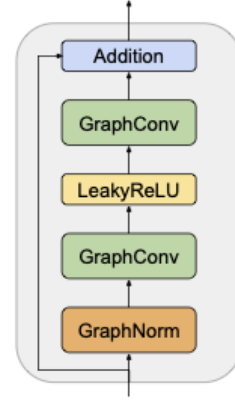


Figure 3. Structure of a residual block in an NSLS.

supplementary convolutional layer increases the receptive field of the neural network earlier.

Normalization Layer. We have compared many normalization layers: instance normalization (Ulyanov et al., 2016), layer normalization (Ba et al., 2016), graph normalization (Cai et al., 2021), graph size normalization (Dwivedi et al., 2020), pair normalization (Zhao & Akoglu, 2019). From our experiments, we see that graph normalization entails consistently the best performances. It is described by the formula

$$\mathbf{x}'_i = \frac{\mathbf{x} - \alpha \cdot \mathbb{E}[\mathbf{x}]}{\sqrt{\text{Var}[\mathbf{x} - \alpha \cdot \mathbb{E}[\mathbf{x}]] + \epsilon}} \cdot \gamma + \beta, \quad (5)$$

where α, β, γ are scalar parameter learned during training.

Convolution Layer. The most common graph convolution layers, like the ones in GraphSAGE (Hamilton et al., 2017), GIN (Xu et al., 2018) or GAT (Veličković et al., 2018), are not suited for weighted graphs. Moreover, the convolutions in classic graph neural networks like GCN (Kipf & Welling, 2017) or GCNII (Chen et al., 2020) can lead to zero division errors with some matrices. Among the graph convolution operators which leverage edge weights, we adopt the GraphConv layer proposed by Morris et al. (2019). The update formula for the GraphConv layer is

$$\mathbf{x}'_i = \Theta_1 \mathbf{x}_i + \Theta_2 \sum_{j \in \mathcal{N}(i)} a_{ji} \mathbf{x}_j, \quad (6)$$

where $\mathbf{x}_i \in \mathbb{R}^d$ is the i -th node feature vector, $\Theta_1, \Theta_2 \in \mathbb{R}^{d' \times d}$ are the parameters of the layer, and a_{ji} denotes the edge weight from source node j to target node i .

Equation (6) shows that the message aggregation function is the sum. In the graph neural network literature many aggregation functions are advocated: for example, mean (Kipf & Welling, 2017), max (Hamilton et al., 2017), softmax and power mean (Li et al., 2020). Here we choose the

sum aggregation function because, thanks to this choice, the message aggregation reduces to a matrix multiplication between the scaled coefficient matrix \bar{A} and the processed node features $F \in \mathbb{R}^{n \times d}$. This choice is straightforward since the workhorse of many iterative methods is the matrix multiplication between the coefficient matrix and vectors depending on \mathbf{b} .

4.4. Loss Function

The output of the GCN is a scale-independent vector, so we are just interested in its direction. For this reason we train the model with the cosine distance loss function:

$$\mathcal{L}_{\cos}(\tilde{\mathbf{x}}, \mathbf{x}) = 1 - \frac{\langle \tilde{\mathbf{x}}, \mathbf{x} \rangle}{\|\tilde{\mathbf{x}}\|_2 \|\mathbf{x}\|_2}. \quad (7)$$

Surprisingly, this loss is not sufficient to recover a good approximation. We have observed that the vectors $\bar{A}\tilde{\mathbf{x}}$ and $\bar{\mathbf{b}}$ can be near-orthogonal even if the angle between $\tilde{\mathbf{x}}$ and \mathbf{x} is tiny. This phenomenon happens because the transformation induced by an ill-conditioned matrix skews angles. To counteract this phenomenon, we use a complementary cosine distance loss on the vectors transformed by \bar{A} :

$$\mathcal{L}_{\text{res}}(\tilde{\mathbf{x}}, \mathbf{x}) = \mathcal{L}_{\cos}(\bar{A}\tilde{\mathbf{x}}, \bar{\mathbf{b}}) = 1 - \frac{\langle \bar{A}\tilde{\mathbf{x}}, \bar{\mathbf{b}} \rangle}{\|\bar{A}\tilde{\mathbf{x}}\|_2 \|\bar{\mathbf{b}}\|_2}. \quad (8)$$

The minimization of \mathcal{L}_{res} ensures that the projection of $\bar{A}\tilde{\mathbf{x}}$ on $\bar{\mathbf{b}}$ does not collapse into the null vector, making the estimation of $\tilde{\mu}$ unreliable.

In conclusion, our full loss function is

$$\mathcal{L}(\tilde{\mathbf{x}}, \mathbf{x}) = \mathcal{L}_{\cos}(\tilde{\mathbf{x}}, \mathbf{x}) + \mathcal{L}_{\text{res}}(\tilde{\mathbf{x}}, \mathbf{x}). \quad (9)$$

5. Experiments

5.1. Results

Dataset. The most used collections of sparse matrices are the Matrix Market (Boisvert et al., 1997) and the SuiteSparse matrix collection (Davis & Hu, 2011). They contain sparse matrices from many engineering problems, but these datasets are too small to train a deep learning algorithm on them. Furthermore, no constant term is reported in conjunction with these matrices. While simulating the solution is a viable option, it entails unrealistic linear systems.

The only public dataset of symmetric sparse linear systems we have found is the StAnD (Grementieri & Finelli, 2022). This dataset contains several solved linear systems originating in the stability analysis of a structure subjected to realistic loads. StAnD problems are divided by size: we perform our experiments on StAnD Small, the subset of linear systems with small coefficient matrices. Besides, we also conduct our experiments on a synthetic dataset generated

using the same matrices from StAnD Small but with solution elements uniformly sampled from $[-1, 1]$. Our tests reveal very different behaviors induced by the two datasets, even if they share the same coefficient matrices. The elements in StAnD Small solution vectors range many orders of magnitudes (from 10^{-16} to 10^{-1}), and we acknowledge this as the cause of the discrepancy.

The matrices in StAnD Small have an average dimension of 2115 rows and columns; this dimension corresponds to the number of nodes in the input system graph. Whereas the size of the system affects the execution time, the graph diameter conditions the precision of an NSLS: indeed, every node should collect information from every other node in its connected component. An NSLS can gather all values in \mathbf{b} , necessary to produce the solution when the inverse of A is dense, only if this condition holds. Otherwise, if the diameter of the system graph is larger than the receptive field of the message-passing neural network at the core of an NSLS, we know that the network has no theoretical possibility to produce a perfect solution. The receptive field of graph neural network depends on the connectivity of the input graph, but in the worst-case scenario of a linear graph it is equivalent to the number of convolution layers in the GCN. The matrices in StAnD Small have an average diameter of about 20, so our models should have at least 20 convolution layers to be expressive enough.

Implementation. All models are implemented using PyTorch Geometric (Fey & Lenssen, 2019). Our models have 10 residual blocks to guarantee a sufficiently wide receptive field since every residual block contains two GraphConv layers. The inner feature dimension d is 32 (small) or 128 (medium), and the training lasts for 50 epochs, or about 315.000 steps using a batch size of 16. We adopt the Adam optimizer (Kingma & Ba, 2014) with no additional regularization. Indeed, we find that regularization is detrimental for such a regression task. We utilize a learning rate $\lambda = 10^{-3}$ at the beginning of the training, dividing it by 10 after 40 and 45 epochs.

Evaluation. We evaluate our models computing on the test set the average of the mean absolute element-wise error ϵ and of the relative approximation error δ with respect to the ground-truth solution $\mathbf{x} \in \mathbb{R}^n$ defined as

$$\epsilon(\hat{\mathbf{x}}, \mathbf{x}) = \frac{\|\mathbf{x} - \hat{\mathbf{x}}\|_1}{n}, \quad \delta(\hat{\mathbf{x}}, \mathbf{x}) = \frac{\|\mathbf{x} - \hat{\mathbf{x}}\|_2}{\|\mathbf{x}\|_2}. \quad (10)$$

The relative error δ is scale-invariant, allowing us to compare models trained on different datasets. On the other hand, the mean absolute element-wise error ϵ tells us how far the approximation actually is from the solution. In practical applications, like structural engineering (the domain of StAnD), we are more interested in the absolute error because the values are associated with a unit of measure, and tiny errors are negligible.

Table 1 compares our leading models trained on synthetic and StAnD Small data. The feature augmentations applied to train such models are diagonal and conjugate gradient augmentations, with 14 steps of the conjugate gradient method to obtain feature vectors of size 16. This combination of features attains the best compromise between accuracy and speed. The results on synthetic data are very satisfactory, exhibiting compelling stability even for the ill-conditioned matrices typical of structural analysis. The relative error on actual StAnD data is much higher because the very low norm of the ground-truth solution distorts it. The absolute error ϵ tells us another story, showing that the approximation is adequately good and the NSLS is sufficiently accurate to replace a classic solver.

Table 1. Evaluation on synthetic and StAnD Small test sets.

DATASET	INNER SIZE	ϵ	δ
SYNTHETIC	$d = 32$	$9.77 \cdot 10^{-3}$	3.40%
	$d = 128$	$8.03 \cdot 10^{-3}$	2.80%
STAND SMALL	$d = 32$	$8.27 \cdot 10^{-6}$	18.28%
	$d = 128$	$5.60 \cdot 10^{-6}$	10.55%

5.2. Ablation Study

In Table 2, we present the results of the ablation study performed to verify the effectiveness of each module of an NSLS. To reduce the running time of experiments, we compare only models with inner feature dimension $d = 32$ on StAnD Small. Even if not specified, we always include the diagonal augmentation.

Table 2. Ablation study on StAnD Small test set.

LOSS	AUGMENTATION	ϵ	δ
\mathcal{L}_{cos}	-	$18.3 \cdot 10^{-6}$	33.93%
$\mathcal{L}_{\text{cos}} + \mathcal{L}_{\text{res}}$	-	$9.01 \cdot 10^{-6}$	21.66%
$\mathcal{L}_{\text{cos}} + \mathcal{L}_{\text{res}}$	ARNOLDI	$8.44 \cdot 10^{-6}$	19.86%
$\mathcal{L}_{\text{cos}} + \mathcal{L}_{\text{res}}$	JACOBI	$8.89 \cdot 10^{-6}$	19.22%
$\mathcal{L}_{\text{cos}} + \mathcal{L}_{\text{res}}$	CG	$8.27 \cdot 10^{-6}$	18.28%
$\mathcal{L}_{\text{cos}} + \mathcal{L}_{\text{res}}$	CG + ARNOLDI	$8.53 \cdot 10^{-6}$	19.04%
$\mathcal{L}_{\text{cos}} + \mathcal{L}_{\text{res}}$	CG + JACOBI	$8.30 \cdot 10^{-6}$	18.12%

The metrics show that the \mathcal{L}_{res} loss is a fundamental component of our architecture. Without this term, the model tends to overfit training data, and the gap between training loss and validation loss increases during the training.

The comparison between feature augmentation strategies shows that all proposed methods improve the final result. As expected, the conjugate gradient augmentation is the most beneficial on positive-definite matrices. On the other hand, Arnoldi iteration, which does not converge to the solution,

is the least effective strategy, and it is also detrimental when combined with conjugate gradient.

5.3. Comparison with Existing Methods

We compare the running time of NSLS with the fastest open-source C++ libraries with GPU support for the resolution of linear systems: cuSOLVER (NVIDIA Corporation, 2022) for direct methods and ViennaCL (Rupp et al., 2016) for iterative algorithms. Since the matrices in StAnD have the additional property to be positive-definite, we compare NSLS with algorithms devised especially for positive-definite systems: Cholesky decomposition (cuSOLVER) and (Preconditioned) Conjugate Gradient (ViennaCL). We remark that our method does not need the additional hypothesis of positive-definiteness. On the contrary, we believe that neural solvers would be much more competitive on general symmetric systems that are harder to solve with classic algorithms. For reference, we also measure the execution time of a pure PyTorch implementation of the conjugate gradient to show that using the same framework and the same amount of user optimizations, NSLSs are faster.

We combine Cholesky decomposition with the fill-in reducing permutation strategies SymAMD (Amestoy et al., 1996), SymRCM (George, 1971) or METIS (Karypis & Kumar, 1998). Similarly, we consider Incomplete Cholesky (Lin & Moré, 1999) and Incomplete LU (Meijerink & Van Der Vorst, 1977) preconditioning to foster the convergence of the conjugate gradient method.

Direct methods cannot exchange accuracy for execution time, so they always reach a very low error. For iterative methods, we record the time needed to reach a relative error equivalent to the one incurred by the NSLS models listed in Table 1. The execution time is measured on a GPU Nvidia GeForce GTX 1080 Ti.

Table 3. Execution time needed by solvers to reach the average relative error δ of the best NSLS with $d = 32$ on synthetic and StAnD Small test data.

ALGORITHM	VARIANT	SYNTHETIC TIME (ms)	STAND SMALL TIME (ms)
CHOLESKY (CUSPARSE)	-	41.9	42.1
	SYMAMD	35.3	35.3
	SYMRM	36.1	36.7
	METIS	31.2	31.1
CONJUGATE GRADIENT (VIENNA CL)	-	2.16	0.84
	ICC	1.97	1.20
	ILU	2.49	1.77
CONJUGATE GRADIENT (PYTORCH)	-	38.1	14.4
NSLS	$d = 32$	13.2	13.4
	$d = 128$	18.7	18.5

NSLSs are still slower than iterative methods, but they enjoy a better utilization of GPU resources and a higher degree of parallelization, as can be seen from the comparison with the pure PyTorch implementation of conjugate gradient. Moreover, the implementation of NSLS in deep learning frameworks like PyTorch (Paszke et al., 2019) or TensorFlow (Abadi et al., 2016) makes these models hardware-agnostic and highly optimized without much effort. We are sure that the inference time of neural solvers will be further reduced by the development of technology. Many research papers already propose more optimized implementations of the sparse matrix multiplication on GPU (Huang et al., 2020), and deep learning frameworks are actively adding support for advanced sparse formats and operations. Anyway, many burdens persist: for example, many neural compilers, like Apache TVM (Chen et al., 2018), do not support variable-size inputs, and thus the optimization of graph neural networks is challenging. Furthermore, the ONNX (Bai et al., 2022) support for sparse operation is very recent (see ONNX opset 16), and accelerators like ONNX Runtime (ONNX Runtime developers, 2022) still have no support for such operations.

5.4. Integration with Iterative Methods

NSLSs provide a coarse approximation of the solution, so they are suited only for non-critical problems where the time constraints are more important than accuracy constraints, for example, in real-time simulations. If more precision is needed, the output of an NSLS can furnish a high-quality initial guess to a classic iterative method. Table 4 shows that the NLSL initialization obtained with the medium model on StAnD Small speeds up the convergence of conjugate gradient, with a substantial reduction in the number of iterations.

Table 4. The average number of iterations needed by the conjugate gradient algorithm to reach a certain relative error on StAnD Small using different initialization vectors.

RELATIVE ERROR δ	ZERO INIT (iterations)	NSLS INIT (iterations)	PERCENTAGE REDUCTION
1%	240	137	-43%
0.1%	362	270	-25%
0.01%	481	395	-18%
0.001%	583	512	-12%

6. Related Works

Graph Representation. Parter (1961) first introduced explicitly the graph representation of a sparse matrix. Rose (1972) pursued a detailed graph-theoretic study of the graph representation for sparse symmetric positive-definite matrices. The graph representation of the matrix is still exploited to design permutation algorithms to reduce the number of

fill-ins in Gaussian elimination. This line of work uses an unweighted graph, and nodes have no features since the graph represents just the matrix of coefficient, not the entire linear system.

Linear System Solvers. Most of the research on linear system solvers focuses on reduced classes of linear systems, like symmetric diagonally dominant (SDD) (Koutis et al., 2012; Spielman & Teng, 2014) or graph-structured (Kyng & Sachdeva, 2016) linear systems. Recently Peng & Vempala (2021) proposed a method asymptotically faster than matrix multiplication applicable to the general case. This last algorithm is comprehensibly very complex, involving many steps and tricks. Unfortunately, no public implementation of the method is available, so it is impossible to test it and measure its actual running time.

Preconditioners. Recent preconditioning methods are specifically designed to be highly parallel and use efficiently GPUs (Anzt et al., 2018; Dziekonski & Mrozowski, 2018; Bernaschi et al., 2019; He et al., 2020; Göbel et al., 2021). Since no preconditioning algorithm works better than others on every matrix, some authors propose to use deep learning to generate the preconditioner matrix (Götz & Anzt, 2018; Sappl et al., 2019; Luna et al., 2021). Preconditioning techniques complement our approach because they improve existing iterative methods, and we have seen how the integration of NSLSs into existing algorithms can reduce the number of iterations.

7. Conclusion

In this work, we present a deep learning model able to solve approximately symmetric sparse linear systems. We test the method on sparse positive-definite linear systems emerging in the field of structural engineering. On this task, the method is not very accurate and slower than classic methods, but the results obtained on a synthetic dataset show the potential capabilities of the model. Moreover, our method suffers from the immaturity of the support for sparse operations in deep learning frameworks. We are confident that the execution time of neural solvers will diminish with further developments of the deep learning libraries.

Overall, our research can be considered a relevant application of a novel general approach to address numerical analysis problems on sparse matrices. For example, we could adapt it to predict an optimal preconditioner matrix for a linear system or an improved initialization for a specific iterative method. Such examples of further developments show the generality of our approach and its flexibility. Since the adaptation of algorithms to the sparse case is challenging and even more troublesome is to parallelize them to use GPUs, we believe that graph neural networks can be an effective alternative to current methods.

References

- Abadi, M., Barham, P., Chen, J., Chen, Z., Davis, A., Dean, J., Devin, M., Ghemawat, S., Irving, G., Isard, M., et al. Tensorflow: a system for large-scale machine learning. In *Proceedings of the 12th USENIX conference on Operating Systems Design and Implementation*, pp. 265–283, 2016.
- Amestoy, P. R., Davis, T. A., and Duff, I. S. An approximate minimum degree ordering algorithm. *SIAM Journal on Matrix Analysis and Applications*, 17(4):886–905, 1996.
- Anzt, H., Huckle, T. K., Bräckle, J., and Dongarra, J. Incomplete sparse approximate inverses for parallel preconditioning. *Parallel Computing*, 71:1–22, 2018.
- Ba, J. L., Kiros, J. R., and Hinton, G. E. Layer normalization. *arXiv preprint arXiv:1607.06450*, 2016.
- Bai, J., Lu, F., Zhang, K., et al. Onnx: Open neural network exchange. <https://github.com/onnx/onnx>, 2022. Version: 1.10.2.
- Battaglia, P. W., Hamrick, J. B., Bapst, V., Sanchez-Gonzalez, A., Zambaldi, V., Malinowski, M., Tacchetti, A., Raposo, D., Santoro, A., Faulkner, R., et al. Relational inductive biases, deep learning, and graph networks. *arXiv preprint arXiv:1806.01261*, 2018.
- Bernaschi, M., Carrozzo, M., Franceschini, A., and Janna, C. A dynamic pattern factored sparse approximate inverse preconditioner on graphics processing units. *SIAM Journal on Scientific Computing*, 41(3):C139–C160, 2019.
- Boisvert, R. F., Pozo, R., Remington, K., Barrett, R. F., and Dongarra, J. J. Matrix market: a web resource for test matrix collections. In *Quality of Numerical Software*, pp. 125–137. Springer, 1997.
- Bronstein, M. M., Bruna, J., LeCun, Y., Szlam, A., and Vandergheynst, P. Geometric deep learning: going beyond euclidean data. *IEEE Signal Processing Magazine*, 34(4): 18–42, 2017.
- Cai, T., Luo, S., Xu, K., He, D., Liu, T.-y., and Wang, L. Graphnorm: A principled approach to accelerating graph neural network training. In *International Conference on Machine Learning*, pp. 1204–1215. PMLR, 2021.
- Chen, M., Wei, Z., Huang, Z., Ding, B., and Li, Y. Simple and deep graph convolutional networks. In *International Conference on Machine Learning*, pp. 1725–1735. PMLR, 2020.
- Chen, T., Moreau, T., Jiang, Z., Shen, H., Yan, E. Q., Wang, L., Hu, Y., Ceze, L., Guestrin, C., and Krishnamurthy, A. Tvm: end-to-end optimization stack for deep learning. *arXiv preprint arXiv:1802.04799*, 2018.
- Davies, A., Veličković, P., Buesing, L., Blackwell, S., Zheng, D., Tomašev, N., Tanburn, R., Battaglia, P., Blundell, C., Juhász, A., et al. Advancing mathematics by guiding human intuition with ai. *Nature*, 600(7887):70–74, 2021.
- Davis, T. A. and Hu, Y. The university of florida sparse matrix collection. *ACM Trans. Math. Softw.*, 38(1), 2011. ISSN 0098-3500. URL <https://doi.org/10.1145/2049662.2049663>.
- Dwivedi, V. P., Joshi, C. K., Laurent, T., Bengio, Y., and Bresson, X. Benchmarking graph neural networks. *arXiv preprint arXiv:2003.00982*, 2020.
- Dziekonski, A. and Mrozowski, M. Block conjugate-gradient method with multilevel preconditioning and gpu acceleration for fem problems in electromagnetics. *IEEE Antennas and Wireless Propagation Letters*, 17(6):1039–1042, 2018.
- Fey, M. and Lenssen, J. E. Fast graph representation learning with pytorch geometric. *arXiv preprint arXiv:1903.02428*, 2019.
- George, J. A. *Computer implementation of the finite element method*. Stanford University, 1971.
- Göbel, F., Grützmacher, T., Ribizel, T., and Anzt, H. Mixed precision incomplete and factorized sparse approximate inverse preconditioning on gpus. In *European Conference on Parallel Processing*, pp. 550–564. Springer, 2021.
- Götz, M. and Anzt, H. Machine learning-aided numerical linear algebra: Convolutional neural networks for the efficient preconditioner generation. In *2018 IEEE/ACM 9th Workshop on Latest Advances in Scalable Algorithms for Large-Scale Systems (scalA)*, pp. 49–56. IEEE, 2018.
- Grementieri, L. and Finelli, F. Stand: A dataset of linear static analysis problems. *arXiv preprint arXiv:2201.05356*, 2022.
- Hamilton, W. L., Ying, R., and Leskovec, J. Inductive representation learning on large graphs. In *Proceedings of the 31st International Conference on Neural Information Processing Systems*, pp. 1025–1035, 2017.
- He, G., Yin, R., and Gao, J. An efficient sparse approximate inverse preconditioning algorithm on gpu. *Concurrency and Computation: Practice and Experience*, 32(7):e5598, 2020.
- Huang, G., Dai, G., Wang, Y., and Yang, H. Ge-spmv: General-purpose sparse matrix-vector multiplication on gpus for graph neural networks. In *SC20: International Conference for High Performance Computing, Networking, Storage and Analysis*, pp. 1–12. IEEE, 2020.

- Karypis, G. and Kumar, V. A fast and high quality multilevel scheme for partitioning irregular graphs. *SIAM Journal on Scientific Computing*, 20(1):359–392, 1998.
- Kingma, D. P. and Ba, J. Adam: A method for stochastic optimization. *arXiv preprint arXiv:1412.6980*, 2014.
- Kipf, T. N. and Welling, M. Semi-supervised classification with graph convolutional networks. In *International Conference on Learning Representations (ICLR)*, 2017.
- Koutis, I., Miller, G. L., and Peng, R. A fast solver for a class of linear systems. *Communications of the ACM*, 55(10):99–107, 2012.
- Kyng, R. and Sachdeva, S. Approximate gaussian elimination for laplacians-fast, sparse, and simple. In *2016 IEEE 57th Annual Symposium on Foundations of Computer Science (FOCS)*, pp. 573–582. IEEE, 2016.
- Lample, G. and Charton, F. Deep learning for symbolic mathematics. In *International Conference on Learning Representations*, 2019.
- Li, G., Muller, M., Thabet, A., and Ghanem, B. Deepgcns: Can gcns go as deep as cnns? In *Proceedings of the IEEE/CVF International Conference on Computer Vision*, pp. 9267–9276, 2019.
- Li, G., Xiong, C., Thabet, A., and Ghanem, B. Deepergcn: All you need to train deeper gcns. *arXiv preprint arXiv:2006.07739*, 2020.
- Lin, C.-J. and Moré, J. J. Incomplete cholesky factorizations with limited memory. *SIAM Journal on Scientific Computing*, 21(1):24–45, 1999.
- Logan, D. L. *A first course in the finite element method*. Cengage Learning, 2016.
- Luna, K., Klymko, K., and Blaschke, J. P. Accelerating gmres with deep learning in real-time. *arXiv preprint arXiv:2103.10975*, 2021.
- Meijerink, J. A. and Van Der Vorst, H. A. An iterative solution method for linear systems of which the coefficient matrix is a symmetric m-matrix. *Mathematics of computation*, 31(137):148–162, 1977.
- Morris, C., Ritzert, M., Fey, M., Hamilton, W. L., Lenssen, J. E., Rattan, G., and Grohe, M. Weisfeiler and leman go neural: Higher-order graph neural networks. In *Proceedings of the AAAI Conference on Artificial Intelligence*, volume 33, pp. 4602–4609, 2019.
- NVIDIA Corporation. cusolver. <https://docs.nvidia.com/cuda/cusolver/>, 2022. Version: 11.6.0.
- ONNX Runtime developers. Onnx runtime. <https://onnxruntime.ai/>, 2022. Version: 1.10.1.
- Parter, S. The use of linear graphs in gauss elimination. *SIAM review*, 3(2):119–130, 1961.
- Paszke, A., Gross, S., Massa, F., Lerer, A., Bradbury, J., Chanan, G., Killeen, T., Lin, Z., Gimelshein, N., Antiga, L., Desmaison, A., Kopf, A., Yang, E., DeVito, Z., Raison, M., Tejani, A., Chilamkurthy, S., Steiner, B., Fang, L., Bai, J., and Chintala, S. Pytorch: An imperative style, high-performance deep learning library. In Wallach, H., Larochelle, H., Beygelzimer, A., d'Alché-Buc, F., Fox, E., and Garnett, R. (eds.), *Advances in Neural Information Processing Systems 32*, pp. 8024–8035. Curran Associates, Inc., 2019.
- Peng, R. and Vempala, S. Solving sparse linear systems faster than matrix multiplication. In *Proceedings of the 2021 ACM-SIAM Symposium on Discrete Algorithms (SODA)*, pp. 504–521. SIAM, 2021.
- Rose, D. J. A graph-theoretic study of the numerical solution of sparse positive definite systems of linear equations. In *Graph theory and computing*, pp. 183–217. Elsevier, 1972.
- Rupp, K., Tillet, P., Rudolf, F., Weinbub, J., Morhammer, A., Grasser, T., Jungel, A., and Selberherr, S. Viennacl—linear algebra library for multi-and many-core architectures. *SIAM Journal on Scientific Computing*, 38(5):S412–S439, 2016.
- Saad, Y. and Schultz, M. H. Gmres: A generalized minimal residual algorithm for solving nonsymmetric linear systems. *SIAM Journal on scientific and statistical computing*, 7(3):856–869, 1986.
- Sappl, J., Seiler, L., Harders, M., and Rauch, W. Deep learning of preconditioners for conjugate gradient solvers in urban water related problems. *arXiv preprint arXiv:1906.06925*, 2019.
- Spielman, D. A. and Teng, S.-H. Nearly linear time algorithms for preconditioning and solving symmetric, diagonally dominant linear systems. *SIAM Journal on Matrix Analysis and Applications*, 35(3):835–885, 2014.
- Ulyanov, D., Vedaldi, A., and Lempitsky, V. Instance normalization: The missing ingredient for fast stylization. *arXiv preprint arXiv:1607.08022*, 2016.
- Van der Vorst, H. A. Bi-cgstab: A fast and smoothly converging variant of bi-cg for the solution of nonsymmetric linear systems. *SIAM Journal on scientific and Statistical Computing*, 13(2):631–644, 1992.

Veličković, P., Cucurull, G., Casanova, A., Romero, A., Liò, P., and Bengio, Y. Graph attention networks. In *International Conference on Learning Representations*, 2018.

Xu, K., Hu, W., Leskovec, J., and Jegelka, S. How powerful are graph neural networks? In *International Conference on Learning Representations*, 2018.

Yannakakis, M. Computing the minimum fill-in is np-complete. *SIAM Journal on Algebraic Discrete Methods*, 2(1):77–79, 1981.

Zhao, L. and Akoglu, L. Pairnorm: Tackling oversmoothing in gnns. In *International Conference on Learning Representations*, 2019.